

Adaptive correction of turbulent distortions by MEMS flexible mirror

L.V. Antoshkin^a, N.V. Goleneva^{ab}, V.V. Lavrinov^{*a1}, L.N. Lavrinova^a

^a V.E. Zuev Institute of Atmospheric Optics SB RAS, 1, Academician Zuev square, Tomsk, 634021, Russia; ^bTomsk State University, 36, Lenina Avenue, Tomsk, 634050, Russia

ABSTRACT

In astronomy, there is a very important task - distortion correction. The problem is solved by an adaptive mirror with a variable geometry which can be created based on MEMS. The annex to the adaptive optics, MEMS is membrane mirror of small dimensions, but with a large number of controls. The action of external forces on the controls adjusts the mirror surface shape correction for distortion compensation. Force directed at one control element slightly affects the shape of the mirror surface in the areas where the remaining elements. It is shown that for each control of the mirror can be affected, which is proportional to the calculated value of the sensor by measuring the wavefront coming to the input aperture of the system.

Keywords: adaptive optics, flexible mirror, turbulent atmosphere

1. INTRODUCTION

Today, with the MEMS associated technological breakthrough that will make mankind in the XXI century. They predict that make the same revolution that made in the XX century microelectronics. Microelectromechanical systems, or MEMS for short - is a set of microdevices wide variety of designs and purposes, produced by methods similar to the use of technological methods of microelectronics. In the world they are known by the acronym MEMS - MicroElectroMechanical Systems. They are united by two features. First - is the presence of moving parts and the purpose of mechanical actions, the second - the size. In studying of microsystems the effects proportional downsizing is particular interest. It is assumed that all dimensions and angles are in a fixed relationship to each other, and only the scale length is changed, for example, isometric scale. Mechanical processes are described by the relevant characteristic values, which should remain constant, so that the process remains the same. Some of the characteristic values depend on the size of the system, while others are independent of it. For example, an elastic vibration scale oscillation frequency is inversely proportional to length. It follows that the mechanical microsystems have a very high natural frequency,

*lvv@iao.ru; phone (3822) 491372; fax (3822) 492086

¹This work was supported by a grant from the Russian Science Foundation №15-19-20013

and thus exhibit significantly improved dynamic performance and lower latency. The adaptive optics MEMS mirror is a membrane of small size but with a sufficiently large number of controls. An illustrative example of the use of a deformable mirror made by MEMS technology, is a deformable mirror Multi-DM, set in the automatic system of laser adaptive optics Robo-AO 1.5-meter telescope at the Palomar Observatory [1, 2]. The mirror 140 is composed of active elements, i.e. Matrix - 12x12 without angular elements. The response time is about 20 microseconds, with no hysteresis. This mirror can be used for wavefront reconstruction in optical systems of various purpose (astronomical optics, microscopy, medicine, remote sensing), including profiling of laser beams, the modulation of the light fluxes, etc. MEMS - technology makes it possible to minimize the interference of neighboring elements, which makes it possible to carry out a complex wavefront correction using Zernike polynomials of high orders. You can create arrays of thousands of items. MEMS - devices manufactured using standard semiconductor processes, which makes it possible to reduce the cost of production and reduce costs.

Microelectromechanical (MEMS) deformable mirror [2] - light with low power consumption deformable mirrors are active aperture to 25.2 mm, consisting of a thin silicon diaphragm controlled array of electrostatic actuators, the number of which varies from 140 to 4092, and which does not have hysteresis. The continuous membrane deformable mirrors are covered with a metal film with highly reflective. Deviation range drive up to 6 μm , the standard error does not exceed 10 nm. An important advantage of the deformable mirror type CDM, created on MEMS technology, in comparison with the bimorph mirror [3 - 6] is the fact that the force acting on one control element slightly affects the shape of the mirror surface in the areas where the other controls. This allows calculate the specific values of the forces acting on each of the controls. On each control mirror may be affected, which is proportional to the value of the wavefront, coming to the input aperture of the adaptive optical system (AOS). The value is determined by the wavefront measurement by Shack-Hartmann wavefront sensor [7, 8], and may include a prediction that built using a Kalman filter to the measured data [9 - 12].

2. FEATURES OF CORRECTION OF TURBULENT DISTORTIONS FLEXIBLE MIRROR TYPE CDM

To implement the correction of turbulent distortions flexible mirror created by MEMS technology (Fig. 4a), is necessary to draw a clear optical harmonization center of the mirror with the center of the lensarray (Fig. 4b) constituting the optical part of Shack-Hartmann WFS and determine the coefficients of the transfer functions. Fig. 1 is a schematic view mirror type CDM.

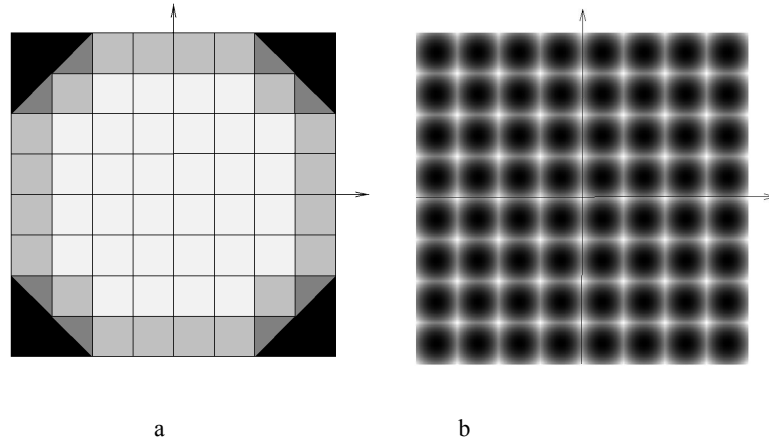


Fig.1. Sketches of the mirror type CDM (a) and lens array optical element as a part of the Shack-Hartmann sensor (b).

The size of the active aperture of the flexible mirror type CDM, created by MEMS technology, is 2.25 mm to 2.25 mm. Mirror has a 32 control ($N_{act} = 32$), with a rectangular configuration placement. Size microactuators - 375 microns to 375 microns. The membrane is made of aluminum. The range of deviations - within 5.5 microns. RMS error is 15.51 nm.

Options lens array 8 x 8 microlens ($N_{lens} = 64$) with a numerical aperture of 0.005 and a focal length of 2 mm. Size square subapertures 640 microns by 640 microns and about 1.7 times the size of the mirror microactuators. Measurement error centroid coordinates recorded in the plane of the camera, is 0.15 pixel [13].

The sensor measures the Shack-Hartmann wavefront arriving at the entrance aperture of the adaptive system, in the form of coordinates of the energy centers of gravity of focal spots - centroid coordinates [14]:

$$\xi_k = \frac{\sum_{i=1}^{n_i} i I_i}{\sum_{i=1}^{n_i} \sum_{j=1}^{n_j} I_{ij}}, \quad \eta_k = \frac{\sum_{j=1}^{n_j} j I_j}{\sum_{i=1}^{n_i} \sum_{j=1}^{n_j} I_{ij}}, \quad I_i = \sum_{j=1}^{n_j} I_{ij}, \quad I_j = \sum_{i=1}^{n_i} I_{ij}, \quad (1)$$

where I_{ij} - the measured intensity signal element coordinates i, j ; $i = 1, 2, \dots, n_i$; $j = 1, 2, \dots, n_j$; n_i, n_j - dimension of the subapertures (number of pixels); k - number of subaperture; $k = 1, 2, \dots, N_{lens} \times N_{lens}$. Displacement of the centroid coordinate for the measured wavefront relative to a reference (for example, the average sample frames or gartmannogramm) are proportional to the local slopes of the wavefront.

The reconstruction of the wavefront is a computational process and can be implemented by an algorithm that today there are many, including the algorithms presented in [16 - 18]. The reconstructed wavefront control is used to control a flexible mirror in AOS [18 - 20]. To correct turbulent distortions by flexible mirror created by MEMS technology are needed only values of the wavefront arriving at the entrance aperture of the system as defined in points agreed with dots localization controls.

In these studies, the reconstruction of the wavefront is only used for the analysis of ways of calculating the values of external forces applied to the mirror controls, as measured Shack-Hartmann WFS.

3. CORRECTIVE MIRROR SURFACE MANAGE

Control surface adaptive mirror is implemented on supply voltages controls. The value of the forces is determined by the centroid coordinates to be measured and the reference wavefronts, as well as pre-measured response function of each control.

Information about the wavefront obtained by the Shack-Hartmann WFS, can be written as the difference of the measured centroid coordinate the coordinates subapertures centers or as a local wavefront tilts, or the coefficients of the basis functions in the expansion of the measured wavefront, or the value of its basic functions in the two-dimensional distribution [15]. Calculated from measurements of the sensor voltage, control the flexible mirror, will vary depending on the form in which information is presented on the wavefront. A method of providing information on the wavefront is characterized by the effectiveness of the calculated values.

One of the criteria for evaluating the effectiveness of the methods of calculating the control voltage u_j of the mirror, is the comparison of the method of least squares phase distribution, reconstructed through the expansion of the wave function in a series of Zernike polynomials $Z_i(x, y)$:

$$W(x, y) = \sum_{i=1}^{N_{\text{basis}}} c_i Z_i(x, y) \quad (2)$$

the distribution phase of the mirror surface in the form of an expansion of the wave function in a series in the response function $F_j(x, y)$:

$$\tilde{W}(x, y) = \sum_{j=1}^{N_{\text{act}}} u_j F_j(x, y) \quad (3)$$

Control voltage of the flexible mirror computed solving the system of equations:

$$A \cdot U = B \quad (4)$$

Where, $A = [F_j(x_k, y_k)]$, $B = [W(x_k, y_k)]$, $U = [u_j]$, $j = 1, 2, \dots, N_{\text{act}}$; N_{act} - The number of response functions; $k = 1, 2, \dots, N$; $F_j(x_k, y_k)$, $W(x_k, y_k)$ - values k -th point of the two-dimensional distributions, j -th response function of the reconstructed wavefront, respectively. The number of equations N , for example, may be the same N_{lens} , the number of subapertures in the lensarray.

The results of studies [15], evaluating the effectiveness of the algorithm for calculating the control voltage of the mirror depending on the reporting of the wavefront, showed that the most accurate calculation algorithm mirror control voltages becomes the solution of equations where the matrix A and B elements are the values of two-dimensional distributions of the reconstructed wavefront and response functions (line 3 in Figure 2). And the least accurate, where the matrix A and B elements are the coordinates of centroid displacements measured wavefront relative to a reference (line 2 in Figure 2). Line 1 corresponds to the profile of the wavefront reconstructed from sensor measurements obtained as a

result of field tests of the laser radiation ($\lambda = 0,633$ microns) at atmospheric path length of 100 m. The calculations were conducted on a grid having 512x512 pixels. The reference wavefront is to use the results of averaging the coordinates of centroid sampling.

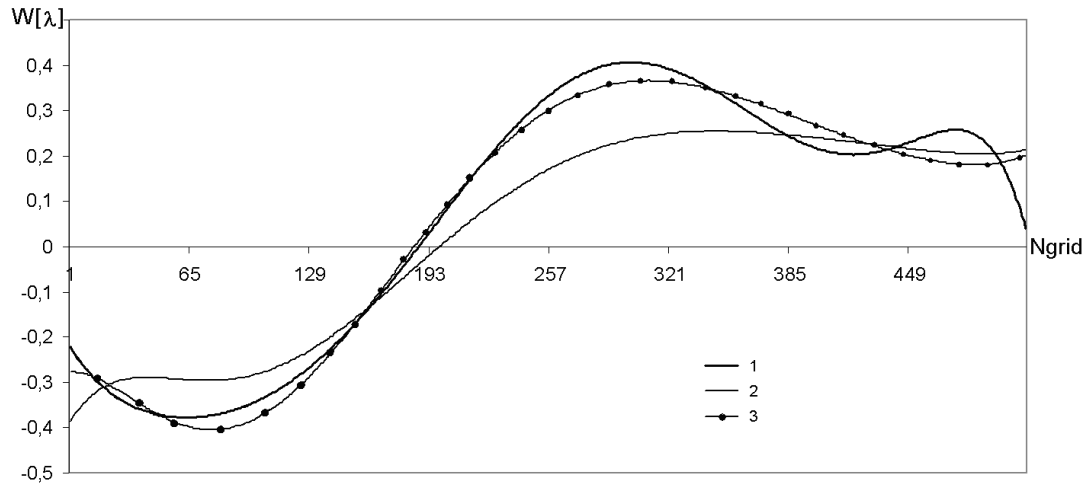


Fig.2. Profile of phase distribution reconstructed from Zernike polynomials (line 1); profiles of the phase of the mirror surface where voltage computed solution of equation (3): line 2 - the matrix and are offset coordinate centroid; 3 - the value of two-dimensional distributions.

The correlation coefficient between the lines 1 and 3 is equal to 0.992591569 and between lines 1 and 2 is 0.9677754888.

4. CALCULATING THE VALUE OF THE WAVEFRONT

The conversion of the light field wavefront sensor Shack-Hartmann can be considered as the transformation of information about it. After passing through the optical field of the lens array with N_{lens} lens size d , information on the field represented by a set of local slopes of the wavefront area or a set of focal spots in the detection plane. The center of gravity of the focal spot corresponds according to the laws of geometrical optics value of the wavefront in the plane, which is a first-order approximation of the wavefront area.

Thus, the value of two-dimensional distributions of the response function $F_j(x_k, y_k)$ and the measured wavefront $\Phi(x_k, y_k)$ at points corresponding to the centers of subapertures, expressed in terms calculated according to (1) coordinate centroid [7]:

$$x'_k = \text{sgn}(-\xi_k) \cdot \frac{d}{2} \cdot \frac{\xi_k^2}{f \cdot \sqrt{f^2 + \eta_k^2 + \xi_k^2}}, y'_k = \text{sgn}(-\eta_k) \cdot \frac{d}{2} \cdot \frac{\eta_k^2}{f \cdot \sqrt{f^2 + \xi_k^2 + \eta_k^2}} \quad (5)$$

$$z'_k = f \cdot \sqrt{\frac{x_k'^2 + y_k'^2}{\xi_k^2 + \eta_k^2}} \quad (6)$$

where f - the focal length; d - the diameter of the subaperture; ξ_k, η_k - coordinates of the centroid k -th subaperture; x'_k, y'_k, z'_k - coordinates of the corresponding point he measured wavefront in the coordinate system of the subaperture.

Regarding lens array coordinates of the measured wavefront x_k, y_k, z_k are defined as follows:

$$\begin{cases} z_k = z'_k + \sum_{i=1}^m z_i^1 + \sum_{i=1}^{m-1} z_i^2, n = 1 \\ z_k = z'_k + \sum_{i=1}^n z_{M \cdot (i-1) + 1}^1 + \sum_{i=1}^{n-1} z_{M \cdot (i-1) + 1}^4 + \sum_{i=2}^m z_{M \cdot (n-1) + i}^1 + \sum_{i=1}^{m-1} z_{M \cdot (n-1) + i}^2, n > 1 \end{cases} \quad (7)$$

where

$$z_k^i = \frac{z'_k \cdot [(p-n) \cdot x_k + (q-m) \cdot y_k - \frac{d}{2} \cdot (p \cdot q - m \cdot n)]}{(p-n) \cdot (m+r \cdot x'_k) + (q-m) \cdot (n+s \cdot y'_k) - \frac{d}{2} (p \cdot q - m \cdot n)}, i = 1, 2, 4 \quad (8)$$

$$x_k = d \cdot [(m-1/2) - M/2]; y_k = d \cdot [(n-1/2) - N/2]. \quad (9)$$

and

- 1) $p = n - 1; q = m + 1; r = 1; s = 1$ if $\xi_k < 0$ and $\eta_k < 0$.
- 2) $p = n - 1; q = m - 1; r = -1; s = 1$ if $\xi_k > 0$ and $\eta_k < 0$.
- 3) $p = n - 1; q = m - 1; r = -1; s = -1$ if $\xi_k > 0$ and $\eta_k > 0$.
- 4) $p = n - 1; q = m + 1; r = 1; s = -1$ if $\xi_k < 0$ and $\eta_k > 0$.

The number $n = \lfloor k/M \rfloor + 1$ indicates the number of rows in the matrix of lenses; $m = k - M \cdot \lfloor k/M \rfloor$ - column number; number of subaperture in the matrix of lens array has form $k = (n-1) \cdot M + m$. $N_{lens} = M \cdot N$ where M - the number of columns in the matrix of lenses, N - the number of lines; $k = 1, 2, \dots, N_{lens}$.

An important requirement for the correction of turbulent distortions mirror implemented by the values of the wavefront, is the fulfillment of the conditions agreed between the optical centers of the correction mirrors and lens array in the Shack-Hartmann sensor. The values z_k of the wavefront coming to the input aperture of the adaptive system are determined by the coordinates in the coordinate system of the mirror, where x_k, y_k - the coordinates that define the position of the centers of subapertures in the plane of the lens array; g_k, h_k - the coefficients of the transfer functions previously calculated for each control of the mirror. The downside correction of turbulent distortions by mirror implemented by the calculated values of the wavefront is a limit: the number of subapertures and the number of controls should be the same. The advantage lies in the simplicity of implementation of predictive control algorithm.

5. THE CONTROL ALGORITHM FLEXIBLE MIRROR USING A KALMAN FILTER

It is known [10] that the surface of the correcting mirror is formed from the surface of the wavefront coming to the input aperture adaptive system deliberately delayed by the amount of delay time of the system. In order to resolve this issue, we proposed the use of the Kalman filter for estimation and predicting of wind offset of the turbulent layer [12]. Kalman

filter, being the optimal linear filter in terms of the mean square approximations [21], leads to the displacement of the wavefront coming to the input aperture of the adaptive system $z_k, k=1,2,\dots,N$ lens. In accordance with the hypothesis of "frozen turbulence" changing the values of the wavefront z_k , there is forward movement, and can be represented by a stochastic differential equation [12]:

$$z_k(i) = z_k(i-1) + \alpha z_k(i-1)\Delta t + E(\Delta t) \quad (10)$$

where $i=1,2,\dots,N$ - with a discrete time interval; $\Delta t, E(\Delta t)$ - an error of the evolution model of the system; α - the variable responsible for the evolution of the system.

Let $\alpha z_k(i-1)\Delta t = U(i-1)$ the effect of atmospheric turbulence in the shear value k -th value of the wavefront.

At the moment i we have inaccurately calculated the value of the wavefront measurement by the uncertainty Shack-Hartmann sensor coordinate centroid:

$$z'_k(i) = z_k(i) + \delta_k(i) \quad (11)$$

where $\delta_k(i) = \delta'_k(i) + \delta''_k(i)$ - a random variable; $\delta'_k(i)$ - coordinates error of the centroid ξ_k ; $\delta''_k(i)$ - a calculating error of the wavefront value.

Using the Kalman Filter (KF shown in Fig. 3), we can get the best value $z_k^{opt}(i)$ closest to the actual value of the wavefront with the delay of the system. For this it is necessary to determine the coefficient K so that the prediction value averaging less likely to differ from the actual values $z_k(i+1)$, ie .:

$$z_k^{opt}(i) = K * z'_k(i) + (1 - K) * (z_k^{opt}(i-1) + U(i-1)) \quad (12)$$

In general, to find the value of the coefficient K , is necessary to minimize the error $\varepsilon_k(i+1)$:

$$\varepsilon_k(i+1) = z_k(i+1) - z_k^{opt}(i+1). \quad (13)$$

Taking into account the equations (10 - 12), we obtain an expression of the form:

$$\varepsilon_k(i+1) = (1 - K) * (\varepsilon_k(i) + E(\Delta t)) - K * \delta_k(i+1). \quad (14)$$

Thus the mean square error will tend to a minimum, ie .:

$$\langle \varepsilon_k^2(i+1) \rangle = (1 - K)^2 * (\langle \varepsilon_k^2(i) \rangle + \sigma_E^2) - K^2 * \sigma_\delta^2 \rightarrow \min \quad (15)$$

then the value of the coefficient Kalman is:

$$K(i+1) = \frac{(\langle \varepsilon_k^2(i) \rangle + \sigma_E^2)}{(\langle \varepsilon_k^2(i) \rangle + \sigma_E^2 + \sigma_\delta^2)} \quad (16)$$

Thus, the optimum predicted value of the wavefront is expressed as follows.:

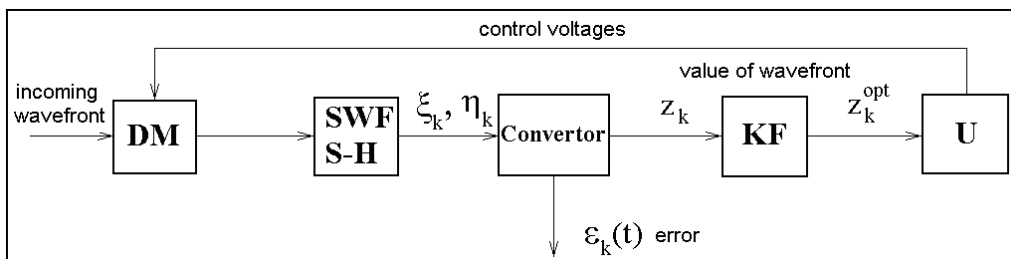


Fig.3. The block diagram of the control algorithm correcting mirror using the Kalman filter applied to calculated by the equations (5 - 9) values of the wavefront.

Kalman filter can be used to estimate the centroid displacement in the recording plane of the S-H wavefront sensor, while forward motion, which make centroid coordinates can be written as an equation [12]:

$$\xi_k(i) = \xi_k(i-1) + \alpha \xi_k(i-1) \Delta t + E(\Delta t) \quad (18)$$

where $i = 1, 2, \dots, N$ - with a discrete time with interval Δt , $E(\Delta t)$ - error model of the evolution of the system, α - characterizing the evolution of the system.

Let $\alpha \xi_k(i-1) \Delta t = U(i-1)$ the real measurement of the sensor $\xi'_k(i) = \xi_k(i) + \delta_k(i)$, where $\delta_k(i)$ - the error of the centroid coordinate ξ_k , then the closest value to the real value of the centroid coordinate with the delay of the system is:

$$\xi_k^{opt}(i) = K * \xi'_k(i) + (1 - K) * (\xi_k^{opt}(i-1) + U(i-1)) \quad (19)$$

The error between the actual and the optimal values of the coordinates of centroid is $\varepsilon_k(i+1) = \xi_k(i+1) - \xi_k^{opt}(i+1)$ or $\varepsilon_k(i+1) = (1 - K) * (\varepsilon_k(i) + E(\Delta t)) - K * \delta_k(i+1)$.

Provided that $\langle \varepsilon_k^2(i+1) \rangle = (1 - K)^2 * (\langle \varepsilon_k^2(i) \rangle + \sigma_E^2) - K^2 * \sigma_\delta^2 \rightarrow \min$ we have a factor $K(i+1)$ of the form (16) and the optimum predicted value of the centroid coordinate as a result of an iterative algorithm:

$$\xi_k^{opt}(i) = K(i) * \xi'_k(i) + (1 - K(i)) * \xi_k^{opt}(i-1) \quad (20)$$

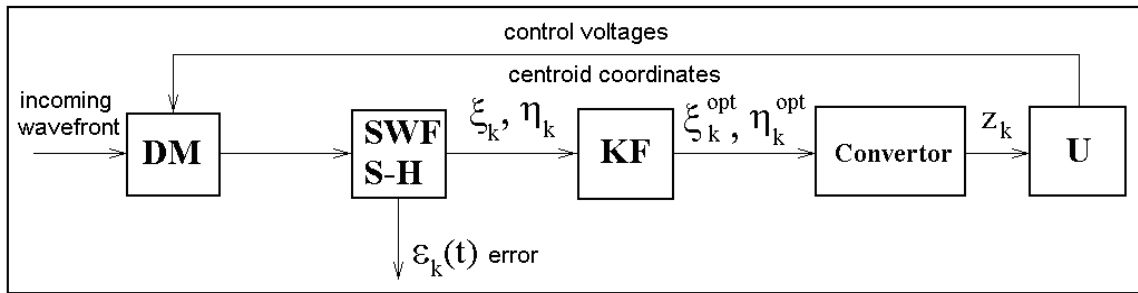


Fig.4. The block diagram of the control algorithm corrective mirror using a Kalman filter applied to the measured sensor centroid coordinates.

In the first method (Fig. 3) error $\varepsilon_k(i+1)$ includes not only the evolution of the model error, but also the coordinates of the centroid of the measurement error, the error calculating the coordinates of the wavefront. In the second method (Figure 4) error calculating the coordinates of the wavefront is not taken into account in the construction of the Kalman filter. Thus, the first method of constructing a Kalman filter is more reliable.

6. CORRECTIVE MIRROR SURFACE MANAGE

The control voltage is determined by the values of the wavefront, and includes prediction constructed by applying the Kalman filter to the values of the wavefront. Relative $\tilde{x}_k = g_k \cdot x_k, \tilde{y}_k = h_k \cdot y_k$ to a mirror coordinate system defined

values $\tilde{z}_k = z_k^{opt}$ of the wavefront (17) corresponding to the incoming time on the entrance aperture of the adaptive system of the wavefront.

The values of the two-dimensional distribution of the response functions z_{jk} do not contain a prediction. The method of least squares fit is performed two-dimensional distribution of the values of the phase of the mirror surface in the form of a series expansion in value of the distribution functions of the response $z_{jk} : \sum_{j=1}^{Nact} u_j \cdot z_{jk}$ the values of the two-dimensional distribution of the wavefront at the entrance aperture of the system \tilde{z}_k , ie, minimized functional of the form:

$$\Psi = \sum_{k=1}^{Nlens} \left\{ \left[\sum_{j=1}^{Nact} u_j \cdot z_{jk} - \tilde{z}_k \right]^2 \right\} \rightarrow \min \quad (21)$$

A necessary condition for an extremum: $\frac{\partial \Psi}{\partial u_j} = 0$. Equation (21) is solved by equating the partial derivatives of the

coefficients of expansion u_j to zero: $\sum_{k=1}^{Nlens} \frac{\partial}{\partial u_j} \left\{ \left[\sum_{j=1}^{Nact} u_j \cdot z_{jk} - \tilde{z}_k \right]^2 \right\} = 0$. As a result of differentiation of the system (21)

takes the form $\sum_{k=1}^{Nlens} \left\{ \left[\sum_{j=1}^{Nact} u_j \cdot z_{jk} - \tilde{z}_k \right] \cdot \sum_{i=1}^{Nact} z_{ik} \right\} = 0$. Since $\sum_{i=1}^{Nact} z_{ik} \neq 0$, $i = 1, 2, \dots, Nact$ in the definition of the

response function, there is a system of $Nlens$ equations $\sum_{j=1}^{Nact} u_j \cdot z_{jk} - \tilde{z}_k = 0$, or

$$\tilde{z}_k = \sum_{j=1}^{Nact} u_j \cdot z_{jk} \quad (22)$$

A sufficient condition for a minimum: $\frac{\partial^2 \Psi}{\partial u_j^2} \geq 0$ ie $\sum_{j=1}^{Nact} z_{jk} \cdot \sum_{i=1}^{Nact} z_{ik} \geq 0$. All values of the response functions are

positive because of their determination. Consequently, $\frac{\partial^2 \Psi}{\partial u_j^2} > 0$ local minimum meet the conditions in the form of

equations (22), which form the matrix of the form (4). The only one solution is a system of the form, $A^T \cdot A \cdot U = A^T \cdot B$ where $A = [z_{jk}]$, $B = [\tilde{z}_k]$, $A^T = [z_{ik}]$, $U = [u_j]$. Elements of the matrix are the values of two-dimensional distributions \tilde{z}_k , z_{jk} calculated by the equations (5 - 9). Control of the mirror voltage is calculated in the usual manner by the matrix: $U = (A^T \cdot A)^{-1} \cdot A^T \cdot B$.

The number of points with coordinates x_k, y_k in the plane of the lensarray, in which the values of the wavefront must be equal to the number of points of application of the voltages u_k in the coordinate system of corrective mirrors: $\tilde{x}_k = g_k \cdot x_k, \tilde{y}_k = h_k \cdot y_k$. Voltages u_k that control of the mirror is determined by the decision of the system of $Nact$ equations (22) at the same time $k = 1, 2, \dots, Nact$. Thus, each control of the correction mirror can be influenced, which is proportional to the value of wavefront that arriving at the entrance aperture of the AOS.

7. CONCLUSIONS

All provisions of the adaptive correction of turbulent distortions by mirror set forth in this paper for flexible mirrors created by MEMS technology can be applied to the management of any corrective phase-conjugate mirror AOS, where the phase is measured by the Shack-Hartmann wavefront sensor.

REFERENCES

- [1] Lewis C. Roberts, Norman A. Page, Rick S. Burruss, Tuan N. Truong, Sharon Dew, Mitchell Troy Conceptual design of the adaptive optics system for the laser communication relay demonstration ground station at Table Mountain, Proc. of SPIE, 8610, 86100N-1-86100N-11(2013).
- [2] Cornelissen S.A., Hartzell A.L., Stewart J.B., Bifano T.G., Bierden P.A. MEMS Deformable Mirrors for Astronomical Adaptive Optics Proc. of SPIE, 7736, 77362D-1 - 77362D-10 (2011).
- [3] Antoshkin L.V., Lavrinov V.V., Lavrinova L.N., Lukin L.V., Tuev M.V. Optimization control active bimorph mirror based Hartmann sensor, Methods and apparatus transmitting and processing information, 11, 25-34(2009).
- [4] Antoshkin L.V., Lavrinov V.V., Lavrinova L.N. Advanced adaptive correction of turbulent distortions based on a Shack-Hartmann wavefront sensor measurements, Optoelectronics, Instrumentation and Data, 48(2), 188-196(2012).
- [5] Antoshkin L.V., Lavrinov V.V., Lavrinova L.N., Lukin L.V. Using photodetectors in Shack-Hartmann wavefront sensors, Optoelectronics, Instrumentation and Data, 48(2), 146-152(2012).
- [6] Sobolev A.S., Cherezova T.Yu., Kudryashov A.V. Analytical and numerical models of a bimorph mirror, Atmospheric and oceanic optics, 18(3), 254-258(2005).
- [7] Lavrinov V.V., Lavrinova L.N., Tuev M.V. Wavefront reconstruction based on the results of light-field conversion by a Shack-Hartmann sensor, Optoelectronics, Instrumentation and Data, 49(3), 305-312(2013).
- [8] Bezuglov D.A., Zabrodin R.A. Method of flexible adaptive piezoceramic mirror approximation by a limited number of Zernike polynomials, Atmospheric and oceanic optics, 19(9), 729-733 (2006).
- [9] Antoshkin L.V., Lavrinov V.V., Lavrinova L.N., Lukin L.V. Methods of forestalling formation of the phase surface on the basis of measurements with the Shack-Hartmann sensor, Atmospheric and Oceanic optics, 24(11), 979-984 (2011).
- [10] Lukin V.P. Dynamic characteristics of adaptive optics systems, Atmospheric and oceanic optics, 23(11), 1027-1035(2010).
- [11] Antoshkin L.V., Lavrinov V.V., Lavrinova L.N., Lukin L.V., Tuev M.V. Peculiarities of forestalling formation of the phase surface on the basis of measurements obtained by the Shack-Hartmann sensor, Atmospheric and Oceanic optics, 23(11), 1042-1047 (2010).
- [12] Lavrinov V.V., Kopylov E.A., Lukin L.V. The development of effective control algorithms with adaptive optical systems for astronomical instruments and laser optoelectronic systems, Proceedings of V Scientific Conference

ОАО “GSKB “Almaz-Antey”, 476-483(2014).

- [13] Lukin V.P., Botygina N.N., Emaleev O.N., Korol'kov V.P., Lavrinova L.N., Nasyrov R.K., Poleshchuk A.G., Cherkashin V.V. Shack-Hartmann sensor based on a low-aperture off-axis diffraction lens array, *Optoelectronics, Instrumentation and Data*, 45(2), 88-98(2009).
- [14] Antoshkin L.V., Lavrinov V.V., Lavrinova L.N., Lukin L.V. Increase of adaptive correction efficiency of turbulent distortions on basis of measurements obtained by the Shack-Hartmann wavefront sensor, *Proc. SPIE*, 8178, 8178OD-1 - 8178OD-9(2011).
- [15] Lavrinov V.V., Lavrinova L.N., Tuev M.V. Numerical simulation of the algorithm to compute the voltage control for the flexible mirror depending on the presentation of information on the wavefront, *Atmospheric and Oceanic optics*, 27(10), 925-931 (2014).
- [16] Maksimov V. G., Tartakovsky V. A., Poleshchuk A. G., Matochkin A. E., Nasyrov R. K. Method for increasing the accuracy of wavefront reconstruction from a set of interferograms, *Optoelectronics, Instrumentation and Data*, 47(6), 593-601(2011).
- [17] Maksimov V.G., Simonova G.V., Tartakovsky V.A. Reconstruction of wavefront with small deformations from a sample of interferograms with different number and orientation interference fringes, *Atmospheric and oceanic optics*, 24(8), 691-697(2011).
- [18] Rukosuev A.L., Kudryashov A.V., Lylova A.N., Samarkin V.V., Sheldakova Yu.V. Adaptive optical system for real-time wavefront correction, *Atmospheric and oceanic optics*, 28(2), 189-195(2015).
- [19] Sheldakova Yu.V., Kudryashov A.V., Rukosuev A.L., Samarkin V.V., Cherezova T.Yu. The use of hybrid algorithm controlling bimorph mirror to focus light radiation, *Atmospheric and oceanic optics*, 20(4), 342-344(2007).
- [20] Kopylov E.A., Lukin V.P. Static characteristics of the DM2-100-31 bimorph mirror and a possibility of its application in the adaptive optical system of Big Solar Vacuum Telescope, *Atmospheric and oceanic optics*, 23(12), 1111-1113(2010).
- [21] Kalman R. E. A new approach to linear filtering and prediction problems, *Transactions of the ASME-Journal of Basic Engineering*, 82(D), 35-45(1960).